ISSN 0036-0244, Russian Journal of Physical Chemistry A, 2017, Vol. 91, No. 12, pp. 2466–2474. © Pleiades Publishing, Ltd., 2017.
Original Russian Text © T.A. Lozinova, A.V. Lobanov, A.V. Lander, 2017, published in Zhurnal Fizicheskoi Khimii, 2017, Vol. 91, No. 12, pp. 2146–2154.

PHOTOCHEMISTRY AND MAGNETOCHEMISTRY

Effect of Na^+ and Ca^{2+} Ions on the Photochemical Formation of Hydrogen Peroxide in Frozen Aqueous Solutions of Adenine Derivatives

T. A. Lozinova[a,*], A. V. Lobanov[b], and A. V. Lander[c]

[a] *Emanuel Institute of Biochemical Physics, Russian Academy of Sciences, Moscow, 119334 Russia*
[b] *Semenov Institute of Chemical Physics, Russian Academy of Sciences, Moscow, 119991 Russia*
[c] *Institute of Earthquake Prediction Theory and Mathematical Geophysics, Russian Academy of Sciences, Moscow, 113556 Russia*
**e-mail: fepr@sky.chph.ras.ru*

Received January 18, 2017

Abstract—The content of hydrogen peroxide is determined in NaCl-containing (0.001–0.1 M) aqueous solutions of adenosine-5'-diphosphate (ADP) and adenosine (Ado) irradiated with near-UV light at 77 K. The obtained data are compared to estimates of the integral intensity (Int) of the EPR signals from the irradiated solutions prior to their thawing and the contents of different components in these spectra (including peroxyl free radicals), calculated by analyzing these spectra from their modeling. It is found that at a low content of photosensitizers (2×10^{-4} M), the relationship between $[H_2O_2]$ and Int differs for ADP and Ado (a positive linear correlation in the case of ADP and a decreasing nonlinear dependence for Ado). It is assumed that these differences are due to the combination of two main factors: (1) the difference between the self-association constants (K_{sa}) of ADP and Ado and (2) the effect of the freezing process, during which added NaCl exerts a disaggregating action of the formation of ADP and Ado associates. The relation between $[H_2O_2]$ and the EPR signal characteristics differs for high (1×10^{-3} M) and low (2×10^{-4} M) concentrations of photosensitizers, suggesting there are two paths of hydrogen peroxide formation in the investigated systems. According to the first path, H_2O_2 is formed during thawing as a result of interaction between peroxyl radicals $O_2^{-\bullet}$ and $HO_2^{\bullet}$ that accumulate during irradiation. According to the second path, the formation of H_2O_2 is direct (without releasing peroxyl radicals into the medium). This probably occurs inside aggregates of adenine derivatives, which form upon freezing the solution. In both cases, adding $CaCl_2$ to test solutions of Ado and ADP ($[CaCl_2] = 0.1–0.2 \times [NaCl]$) results in a substantial drop in the yield of H_2O_2.

Keywords: adenine derivatives, photolysis, hydrogen peroxide, EPR, peroxyl radicals

DOI: 10.1134/S0036024417120160

INTRODUCTION

It was shown in [1, 2] that hydrogen peroxide can be found in samples obtained by thawing aqueous solutions of adenine derivatives AX (where X is H for adenine (A), ribose for adenosine (Ado), and ribose-5'-diphosphate for adenosine-5'-diphosphate (ADP)) irradiated with near-UV light at 77 K. The formation of H_2O_2 in Ado samples intensifies in the presence of NaCl [1]. There is no H_2O_2 in similarly irradiated samples of guanosine-5'-monophosphate and thymine, but trace amounts of it can be found in cytidine solutions. The content of hydrogen peroxide has been determined in solutions of the derivatives of different nucleic acid bases at a relatively high content of them (1×10^{-3} M) after irradiating these solutions under identical conditions in the presence of NaCl (0.1 M) [2]. Based on a comparison of the obtained results, it was assumed that the observed uniqueness of AX derivatives in terms of the photoproduction of H_2O_2 could be due to their associative properties [2].

A comparison of the results from determining H_2O_2 in AX samples irradiated at the wavelengths of their absorption bands (λ = 240–400 nm) and the results from analyzing the EPR spectra recorded for the irradiated samples before thawing suggests that H_2O_2 in the investigated systems could form via the reaction

$$O_2^{-\bullet} + HO_2^{\bullet} + H_2O \rightarrow H_2O_2 + O_2 + OH^-. \quad (1)$$

The formation of free radicals $O_2^{-\bullet}$ and $HO_2^{\bullet}$ in the investigated systems is confirmed by their EPR spectra

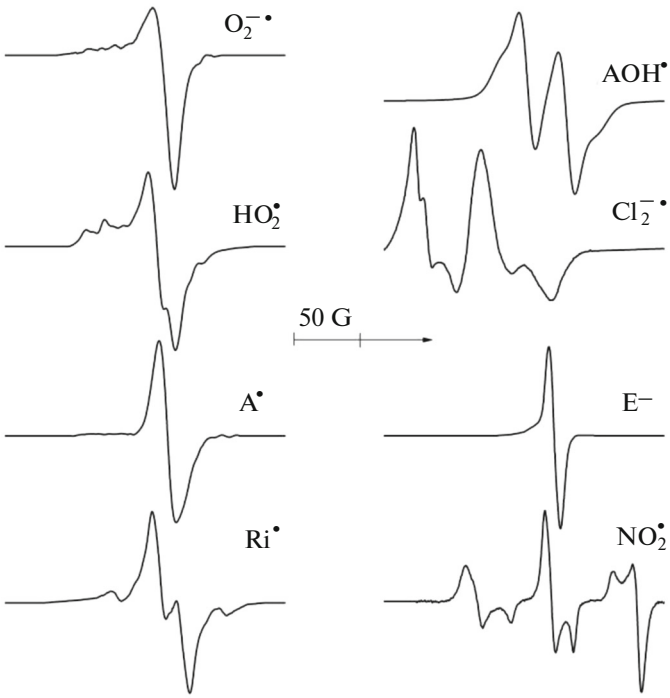

Fig. 1. Main basic spectra used in modeling the EPR signals of adenine derivatives.

obtained at 77 K and analyzed via their modeling [3, 4], which is similar to the method used in this work.

The aims of this work are

(a) to compare the results from determining the photoinduced formation of hydrogen peroxide and analyzing the EPR spectra of NaCl-containing solutions of ADP and Ado to data obtained earlier, and to analyze the effect of NaCl on the correlation between the photoproduction of H_2O_2 and the signal intensity/composition of the EPR spectra of irradiated solutions of Ado and ADP before thawing;

(b) to analyze the effect of $CaCl_2$ (a presumable complexing agent) on the possible relationship between these values.

EXPERIMENTAL

Our ADP (trisodium salt) came from Sigma; our Ado, from Serva (Germany). Other reagents were of reagent grade. Solutions were prepared using water from a Millipore purification system. All experiments were performed in a weakly acidic medium (pH 6.6). The pH of the solutions was adjusted to this value before freezing by adding HCl and NaOH. The contents of ADP and Ado were 2×10^{-4} M. Control measurements were performed at the higher concentration used in earlier studies, [AX] = 1×10^{-3} M. The content of [NaCl] was varied in the range of $(2–1000) \times 10^{-4}$ M; $CaCl_2$ was added in amounts of $0.1–0.2 \times$ [NaCl]. Samples were frozen in Teflon cartridges via rapid immersion in liquid nitrogen and released from the cartridges immediately before irradiation. Irradiation was performed using a DPSh-1000 high-pressure mercury lamp with UFS-5 light filter (transmission, 240–400 nm). In [2], we observed no dependence of the yield of H_2O_2 on the intensity of irradiation ($I_{h\nu}$) in the range of 0.2–1 at low concentrations of A and Ado, despite the considerable difference between the integral intensities (Int) of the corresponding EPR signals. The intensity of irradiation was therefore limited using gratings calibrated on a spectrophotometer. The $I_{h\nu}$ value was ≈0.6 of the maximum intensity of irradiation. The samples were irradiated at 77 K (in liquid nitrogen) in a quartz Dewar flask. EPR spectra were recorded at 77 K (frequency, 9.5 GHz) on an EPR spectrometer manufactured at our laboratory. The microwave radiation power was $W \approx 200$ μW and $W \approx$ 2 mW. The amplitude of modulation was ~2 G.

A quantitative estimate of the contribution from different components to the total EPR spectra (signals *S*) recorded at g ≈ 2.00 was obtained by constructing a model signal using the DECO_2016 computer simulation software, which is a modification of the versions used earlier. The calculation procedure was described in [4]. The individual (basic) signals from the components that contributed the most to the recorded spectra of irradiated solutions of AX are shown in Fig. 1. These are the signals from (1) peroxyl radicals $O_2^{-\bullet}$; (2) peroxyl radicals $HO_2^\bullet$; (3) radical cations of adenine, most likely in their deprotonated form ($pK_a < 4.2$ [5]);

Table 1. Results from determining H_2O_2 and analyzing the EPR spectra for samples AX + NaCl and AX + NaCl + $CaCl_2$

Compound	Composition of solutions, $M \times 10^4$			$[H_2O_2]$, μM	Int, c.u.	Relative content of components					
	[AX]	[NaCl]	[$CaCl_2$]			$O_2^{-\bullet}$	$HO_2^{\bullet}$	$A^{\bullet}$	$Ri^{\bullet}$	$AOH^{\bullet}$	$Cl_2^{-\bullet}$
ADP	10	1000	–	250	1115	0.212	0.155	0.197	0.207	0.129	0.066
ADP	10	1000	100	33	969	0.244	0.168	0.110	0.287	0.094	0.061
ADP	2	1000	–	190	625	0.252	0.088	0.202	0.106	0.104	0.110
ADP	2	1000	100	26	805	0.342	0.038	0.161	0.195	0.087	0.121
ADP*	2	1000	–	240	962	0.167	0.213	0.184	0.144	0.108	0.121
ADP*	2	1000	100	43	721	0.313	0.000	0.157	0.267	0.074	0.061
ADP	2	10	–	30	169	0.064	0.282	0.156	0.314	0.087	0.014
ADP	2	12	–	39	122	0.107	0.138	0.176	0.300	0.173	0.004
ADP	2	10	2	10	94	0.060	0.121	0.359	0.243	0.124	0.016
ADP	2	–	10	1	113	0.087	0.111	0.285	0.254	0.174	0.000
ADP	2	2	–	15	48	0.103	0.111	0.333	0.079	0.250	0.000
ADP	2	–	2	3	41	0.067	0.127	0.297	0.261	0.204	0.015
Ado	2	1000	–	81[a]	1151[a]	0.237	0.242	0.235	0.140	0.044	0.069
Ado	2	1000	–	110[b]	335[b]	0.143	0.210	0.126	0.270	0.046	0.130
Ado*	2	1000	–	140[b]	413[b]	0.202	0.166	0.226	0.141	0.169	0.059
Ado	2	1000	100	38	787	0.312	0.079	0.177	0.149	0.091	0.133
Ado	2	10	–	145	157	0.000	0.274	0.298	0.191	0.160	0.004
Ado	2	12	–	195	167	0.030	0.258	0.239	0.222	0.151	0.000
Ado	2	10	2	72	177	0.085	0.178	0.236	0.245	0.161	0.000
Ado	2	–	5	45	113	0.065	0.228	0.228	0.296	0.084	0.006
Ado	2	–	10	48	167	0.109	0.215	0.198	0.401	0.000	0.020

Light filter, UFS-5. *Duration of irradiation $t = 32$ min; for other samples, $t = 16$ min. Intensity of irradiation $I_{h\nu} = 0.6$; [a] from [2], $I_{h\nu} = 1$; [b] from [2], $I_{h\nu} = 0.2$. Shown are the average values of the results obtained in parallel experiments.

(4) ribose radicals $Ri^{\bullet}$ in Ado and ADP (these radicals are mainly localized on C5'); (5) C8OH adducts of adenine $AOH^{\bullet}$; (6) $Cl_2^{-\bullet}$, which is present in NaCl-containing solutions; (7) electrons E^- stabilized in the matrix; and (8) $NO_2^{\bullet}$ radicals. The presence of the latter signal in the spectra was probably due to nitrate admixtures in the components of the solutions. Although this signal was clearly visible at the high microwave power (W), the contribution from the signals of $NO_2^{\bullet}$ radicals to signals S at $W \approx 200$ μW normally does not exceed ~5%. The parameters and conditions for obtaining the basic spectra were given in [3, 4] and in the works cited there. In addition to the abovementioned signals, the signal from the Dewar flask was also added to the basic systems.

The yield from different paramagnetic products was determined from the spectra recorded under conditions in which the dependence of the integral intensity of all the components on $W^{1/2}$ was close to linear (W = 200 μW), similarly the same way as in earlier studies.

After the EPR spectra were recorded, the irradiated samples were stored for 24 h in liquid nitrogen before determining the H_2O_2 content. In each experiment, the determination of H_2O_2 was performed in parallel with the irradiated samples for control samples that were not irradiated but were stored for the same time at 77 K.

The quantitative determination of H_2O_2 was performed by spectral-iodometric means [6]. To accomplish this, the samples were thawed at room temperature after photolysis. After measuring their volume, they were supplied with 1 mL H_2SO_4 (0.2 M). Dissolved oxygen was displaced by blowing with CO_2. The samples were then mixed with 2 mL a deaerated 5% potassium iodide water solution and purged with CO_2 once again. The emission of iodine, which forms complex I_3^- anions with excess iodide anions, was detected via spectrophotometry ($\lambda_{max} = 351$ nm, $\varepsilon = 26400$ M^{-1} cm^{-1}).

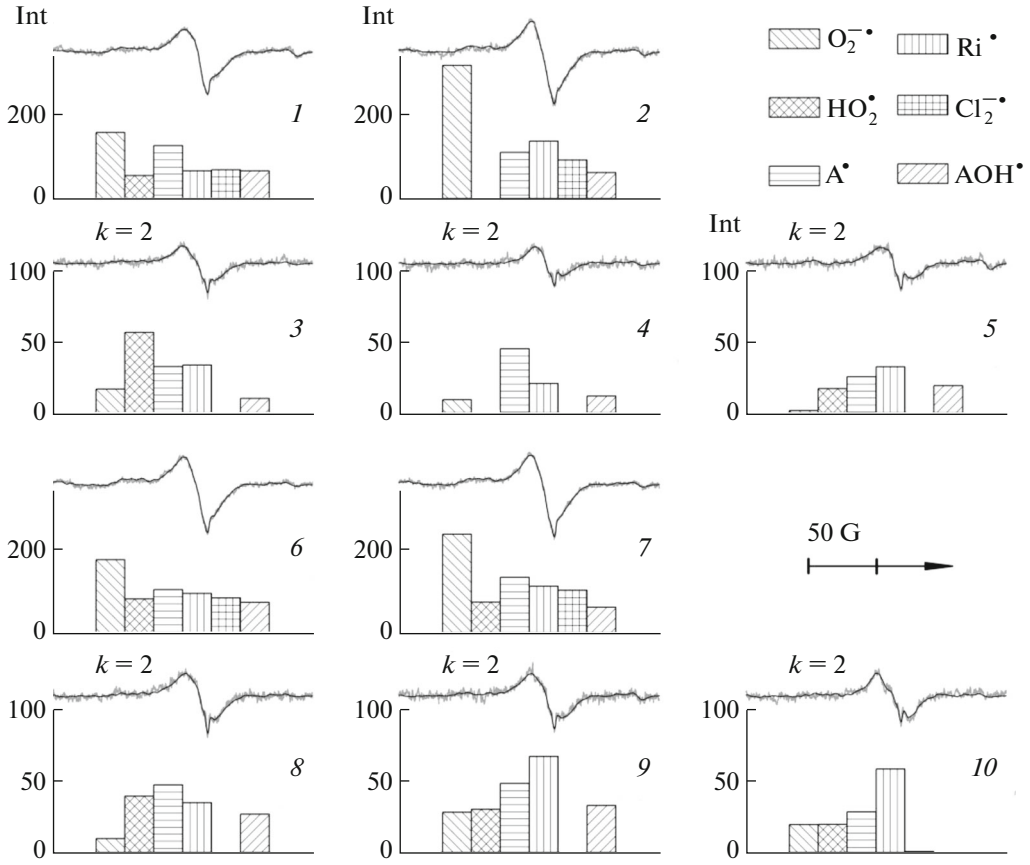

Fig. 2. Examples of EPR spectra registered in irradiated solutions of (*1–5*) ADP and (*6–10*) Ado; [AX] = 2×10^{-4} M. Irradiation was performed with a UFS-5 light filter; $I_{h\nu} = 0.6$. The duration of irradiation was 16 min. The content of additives of inorganic salts was (*1, 6*) [NaCl] = 0.1 M; (*3*) [NaCl] = 0.001 M; (*8*) [NaCl] = 0.0012 M; (*2, 7*) [NaCl] = 0.1 M + [$CaCl_2$] = 0.01 M; (*4*, *9*) [NaCl] = 0.001 M + [$CaCl_2$] = 0.0002 M; and (*5*, *10*) [$CaCl_2$] = 0.001 M. The experimental EPR spectra are represented by gray lines; the model, by black lines. The results from estimating the contribution from the main components of signals (in arbitrary units) are presented under the spectra. $W = 200$ μW.

RESULTS AND DISCUSSION

Table 1 presents the results from determining the hydrogen peroxide content in thawed AX samples irradiated at 77 K. The same table shows the results from determining the integral intensities of the EPR spectra in these samples before thawing (Int) and the results from assessing the contribution from the main components to the registered total spectra. The content of

Table 2. Comparison of the H_2O_2 yield and the Int of the EPR signals for the solutions of AX (1×10^{-3} M) + NaCl after irradiation with a UFS-5 light filter (16 min) and data obtained earlier, along with data from calculating the concentrations of dimeric associates [AX_2] using the values of K_{sa}^{Ado} and K_{sa}^{ADP} in [11, 12] (*) and of K_{sa2}^{Ado}, K_{saN}^{Ado}, K_{sa2}^{ADP}, and K_{saN}^{ADP} in [8, 9] ([a])

[NaCl], M	$I_{h\nu}$	[H_2O_2], μM/Int, c. u.			Reference	[AX_2], μM		
		Ado	ADP	A		Ado	ADP	A
0.1	1	440/1144	–	84/1116	[2]	14*–24**; 408[a]–423[aa]	2*–4**; 359[a]–386[aa]	387[a]–400[aa]
	0.6	–	250/1115	–				
	~0.4	145/900	90/598	–	[1]			
	0.2	350/900	–	45/294	[2]			
0	~0.4	110/79	–		[1]			

Double indices denote the results from calculating [AX_2] while assuming that all values of K_{sa} grow by a factor of 1.8 when the solutions freeze (this value was estimated from the data in [14] for purine solutions).

Table 3. Comparison of the H_2O_2 yield and the Int of the EPR signals in the solutions of AX (2×10^{-4} M) + NaCl after irradiation with a UFS-5 light filter (16 min) and data obtained earlier, plus the data from calculating the concentrations of dimeric associates $[AX_2]$ using the values of K_{sa}^{Ado} and K_{sa}^{ADP} in [11, 12] (*) and of K_{sa2}^{Ado}, K_{saN}^{Ado}, K_{sa2}^{ADP}, and K_{saN}^{ADP} in [8, 9] ([a])

[NaCl], M	I_{hv}	$[H_2O_2]$, μM/Int, c. u.			Reference	$[AX_2]$, μM		
		Ado	ADP	A		Ado	ADP	A
0.1	1	81/1151	–	34/1285	[2]	0.6*–1.1**; 67[a]–74[aa]	0.1*–0.2**; 50[a]–59[aa]	62[a]–69[aa]
	0.6	–	190/625	–				
	0.2	110/335	–	32/239	[2]			
0.0012		195/167	39/122	–				
0.0010	0.6	145/157	30/169	–				
0.0002		–	15/48	–				

Double indices denote the results from calculating $[AX_2]$ while assuming that all values of K_{sa} grow by a factor of 1.8 when the solutions freeze (this value was estimated from the data in [14] for purine solutions).

H_2O_2 in the control samples (the unirradiated samples that were stored for the same time intervals at 77 K) did not exceed 1 μM. Examples of the EPR spectra registered for the irradiated samples at 77 K and the results from their modeling are shown in Fig. 2. It should be noted that the tables show the concentration of added NaCl. Since we used a trisodium salt of ADP, the actual $[Na^+]$ value at low contents of NaCl therefore exceeds those given in the table.

(I) The effect of NaCl. Tables 2 and 3 show the results from comparing measurements of the H_2O_2 yield and the Int of the signals in AX + NaCl systems to data obtained earlier. The yield of H_2O_2 in ADP solutions exceeds that of H_2O_2 in Ado solutions at the relatively low value of $[AX] = 2 \times 10^{-4}$ M and the fairly high value of [NaCl] = 0.1 M. In other cases, the yield of H_2O_2 proves to be higher in Ado solutions than in ADP solutions. We assume that the observed ratios of the H_2O_2 yields in Ado and ADP solutions can be explained by a combination of two main causes:

The first of these is *the difference between the self-association constants (K_{sa}) of Ado and ADP.* The literature data on determining the self-association constants of AX (K_{sa}^{AX}) in liquid solutions (these constants are usually calculated in accordance with the widely accepted isodesmic model, which assumes the identity of all stages of the formation of multidimensional associates) are characterized by an extremely wide spread. (The results from determining the self-association constant for adenosine-5'-triphosphate (ATP), K_{sa}^{ATP}, differ by a factor of more than 60; for adenosine-5'-monophosphate (AMP), the determined K_{sa}^{AMP} values differ by a factor of 7 [7]). It was shown in [8, 9] that, in addition to the differences between possible theoretical models chosen to analyze association, an essential role is played by the working interval of AX concentrations that is available to different experimental methods. For AX, UV spectroscopy has revealed the existence of two hypochromic effects that indicate the association of molecules [8, 9]. The first effect is apparent when $[AX] < 1 \times 10^{-3}$ M; the second effect, at higher [AX]. The authors attribute the observed effect to a substantial (up to two orders of magnitude) increase in the formation constant of the dimeric associates (K_{sa2}), compared to the corresponding value for the formation of associates of higher orders, which is assumed to be the same (K_{saN}). A more complex model that in the case of noncovalent bonds considers the loss of the rotational and translational degrees of freedom of monomeric aromatic single molecules upon their association also shows a sharp drop in K_{sa} when $N \geq 3$ [10].

The values of K_{saN} obtained in [8, 9] approximately correspond to the K_{sa} values calculated using the isodesmic model only in the close range of [AX]. The following K_{sa} values were obtained for Ado and ADP via calculations using the isodesmic model and the NMR data (in D_2O and $NaNO_3$, ionic strength I of solutions is 1): $K_{sa}^{Ado} = 15$ M^{-1} (pD = 7) [11] and $K_{sa}^{ADP} = 1.8$ M^{-1} (pD = 8.9) [12].

A reduction in pH raises the K_{sa} value for nucleotides, which is ~40% of the one obtained at more alkaline pH values [13]. The corresponding values obtained in [8, 9] (0.05 M phosphate buffer, pH 6.9) were $K_{saN}^{Ado} = 120$ M^{-1} and $K_{saN}^{ADP} = 51$ M^{-1}; for second-order associates, $K_{sa2}^{Ado} = 1.6 \times 10^4$ M^{-1} and $K_{sa2}^{ADP} = 0.5 \times 10^4$ M^{-1}.

Tables 2 and 3 show the results from calculating the concentrations of dimeric AX associates (AX_2) in liquid solutions using the K_{sa} values given in the works cited above. In our calculations, we considered the probability of the formation of dimeric and trimeric associates. In both cases, the possibility that K_{sa} will rise as the temperature falls during freezing was also

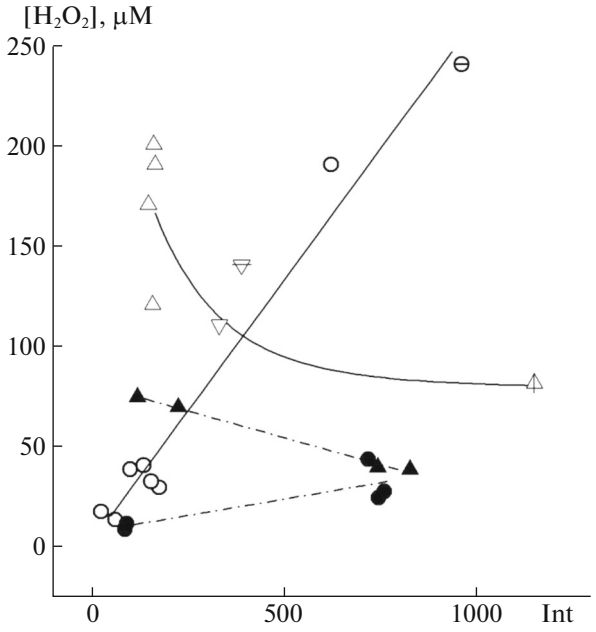

Fig. 3. Correlation between the yield of H_2O_2 and the integral intensity of the EPR signals registered in irradiated solutions of AX + NaCl before thawing. [AX] = 2×10^{-4} M; [NaCl] = 0.001–0.1 M. In the experiments with $CaCl_2$, [$CaCl_2$] = 0.1–0.2 × [NaCl] (Table 1). All samples were irradiated with a UFS-5 light filter. ○ ADP, t = 16 min; ⊖ ADP, t = 32 min; △ Ado, t = 16 min; ● ADP + $CaCl_2$, t = 16 min; ▲ Ado + $CaCl_2$, t = 16 min; $I_{h\nu}$ = 0.6. From [2]: ▽ Ado, t = 16 min, $I_{h\nu}$ = 0.2; ▽ Ado, t = 32 min, $I_{h\nu}$ = 0.2; ⧋ Ado, t = 16 min, $I_{h\nu}$ = 1.

taken into account. For purine solutions (Pu), this rise is as high as ~1.8 as we go from room temperature to 4.9°C [14].

Calculations of [AX_2] upon such a rise in K_{sa} show a significant increase in [AX_2] only when we use the K_{sa} values from [11, 12]. In this case, however, the possible [AX_2] turns out to be much lower than the observed yield of H_2O_2. Calculations of [AX_2] based on the values of K_{sa2} and K_{saN} in [8, 9] give values consistent with the yield of H_2O_2 (Tables 2 and 3).

In [2], it was assumed associates play an important role in the formation of H_2O_2, based on a comparison of our experimental data and the K_{sa} values reported in the literature obtained via NMR for the derivatives of various nucleic bases. Since the K_{sa2} values given in [8, 9] exceed these by more than three orders of magnitude, we must estimate their ratios for different compounds. This is apparently essential when dealing with frozen solutions as well.

According to [11, 15] the K_{sa}^{Ado}/K_{sa}^{Pu} ratio obtained via NMR for Ado and Pu at pH 7 is ~6.5. The $K_{sa2}^{Ado}/K_{sa2}^{Pu}$ and $K_{saN}^{Ado}/K_{saN}^{Pu}$ ratios are ~5.3 and 7.5, respectively. These ratios are quite similar, and if they hold for other compounds, the use of the results from [8, 9] is completely justified.

It should be noted that the determined K_{sa} values depend largely on the content of inorganic salts in the solutions. There are experimental data indicating that in liquid solutions, the complexation of AX with metals promotes stacking interaction between molecules [7, 11, 12, 15–17]. These data apply to both adenine nucleotides and to adenosine [17]. However, the K_{sa} in Ado + NaCl (1 M) solutions is only ~1.2 times higher than in pure aqueous solutions of Ado [17]. For ADP, K_{sa} increases by a factor of 1.3 when a 1 M solution of NaCl is used instead of a 0.1 M NaCl solution. This effect is therefore unlikely to be important in the salt concentration range that we uses (10^{-3}–10^{-1} M).

The second cause is the effect of freezing. This process is apparently the most important (and the most difficult to define) factor for a possible relationship between the yield of H_2O_2 and the association of AX. It is known that the freezing of aqueous solutions of aromatic organic molecules leads to their aggregation. In the presence of inorganic salts, however, these compounds disaggregate [18, 19]. It is assumed that both vertical stacking and horizontal interactions occur during the aggregation of molecules. The degree of aggregation depends on the type of AX molecules, their concentration, and the composition of the solution. The presence of NaCl in the frozen solutions could thus be an important factor in the considered experiments.

A possible relation between the yield of H_2O_2 and the Int of EPR signals from AX + NaCl solutions with rising [NaCl] is shown in Fig. 3. In the case of ADP, the respective correlation was close to linear (coefficient of linear correlation K_{cor} was 0.986). In the case of Ado, however, the dependence of the yield of H_2O_2 on Int is apparently described by a falling curve. (It should be noted that the values provided in this figure for Ado refer to the results obtained at different $I_{h\nu}$.)

Assuming there is a relation between the yield of H_2O_2 and the association of AX, the dependence observed for Ado can apparently be explained by the disaggregating effect of NaCl. This effect is not apparent in ADP solutions, due probably to stronger complexation of Na^+ with the hydroxyls of the phosphate groups of ADP (the formation of ionic bonds between Na^+ and O^-). In [18], luminescent measurements showed that in the case of Ado, the disaggregating effect of NaCl is very apparent even at [NaCl] = 10^{-3} M. Such changes in aggregation cannot be achieved in the nucleotide (AMP) even at [NaCl] = 1 M. The disaggregating effect of NaCl in solutions of A is apparent at intermediate values of [NaCl].

It is obvious that the formation of aggregates in the investigated systems is determined by a combination of two main factors: the self-association of AX and the disaggregating action of NaCl. The assumption that

Table 4. The coefficients of linear correlation (K_{cor}) of the yield of hydrogen peroxide ([H_2O_2]) with EPR signal intensities S (Int), the intensities of signals of radicals [$HO_2^{\bullet}$] and product P = [$O_2^{-\bullet}$] × [$HO_2^{\bullet}$], calculated using the linear relation $y = A + B \times x$

Sample group	n	K_{cor}			R^2_{lin}			R^2_{allo}			Reference
		Int	[$HO_2^{\bullet}$]	P	Int	[$HO_2^{\bullet}$]	P	Int	[$HO_2^{\bullet}$]	P	
Ado + A + ADP	16	0.822	0.924	0.927	0.676	0.854	0.859	0.857	0.930	0.869	[2]
	12	0.874*	0.936*	0.950*	0.764*	0.876*	0.902*	0.944*	0.958*	0.939*	
Ado + A	14	0.865	0.924	0.931	0.748	0.853	0.867	0.860	0.939	0.872	[2]
	10	0.913*	0.935*	0.954*	0.834*	0.874*	0.910*	0.948*	0.971*	0.949*	
Ado + ADP	10	0.825	0.944	0.930	0.681	0.892	0.865	0.861	0.937	0.869	[2]
	8	0.906*	0.952*	0.959*	0.821*	0.906*	0.920*	0.950*	0.961*	0.942*	
Ado	8	0.888	0.941	0.934	0.788	0.886	0.872	0.859	0.940	0.873	[2]
	6	0.946*	0.949*	0.960*	0.895*	0.901*	0.922*	0.959*	0.975*	0.953*	

R^2_{lin} is the coefficient of determination, which coincides with the K^2_{cor} value of linear correlation. R^2_{allo} is the coefficient of determination for allometric dependence $y = C + D \times x^2$, n is the number of points in a group. * The values of the same parameters after excluding samples with [AX] = 2×10^{-4} M; [NaCl] = 0.1 M. The samples were irradiated with a UFS-5 light filter.

the formation of H_2O_2 is related to the association of AX [2] thus does not seem to contradict the literature data.

In [2], it was established for AX solutions (1×10^{-3} M) containing 0.1 M NaCl that the yield of H_2O_2 determined upon thawing the irradiated samples correlated with the content of free radicals $HO_2^{\bullet}$ and the product of [$HO_2^{\bullet}$] × [$O_2^{-\bullet}$] (P), both of which were calculated from the EPR spectra. Most of the data (>70%) provided in [2] were obtained at [AX] = 1×10^{-3} M, which is relatively high. Removing the data corresponding to the low [AX] of 2×10^{-4} M from the results provided in [2] considerably raises the coefficients of linear correlation and determination (Table 4). In contrast to these results, there is no correlation between the yield of H_2O_2 and the content of radicals $HO_2^{\bullet}$ or the P value ($K_{cor} < 0.900$) at [AX] = 2×10^{-4} M (the concentration used in this work), not even in the case of ADP.

We may therefore assume the existence of two paths of hydrogen peroxide formation in the analyzed systems: (1) the formation of H_2O_2 via the interaction of $O_2^{-\bullet}$ and $HO_2^{\bullet}$ radicals (that accumulated during the irradiation) in the process of thawing the solutions and (2) the immediate formation of H_2O_2 during irradiation (possibly inside the aggregates of AX). The second path is also supported by the formation of H_2O_2 in Ado and A solutions (2×10^{-4} M) containing 0.1 M NaCl during the irradiation of samples at λ = 290–450 nm, which encompasses only the long-wavelength absorption region of AX [2]. For the samples irradiated at the low $I_{h\nu}$ of 0.2 for 16 min, the yield of H_2O_2 was 23–29 μM and there were virtually no EPR signals. The quantitative ratio of the peroxide formed in each of these paths seems to be largely determined by the structure of the frozen solutions.

(II) The effect of $CaCl_2$. When setting the aims of this work, we assumed that adding Ca^{2+} ions to the investigated solutions could greatly increase the yield of hydrogen peroxide through the abovementioned promotion of stacking interaction between molecules by metal ions [7, 11, 12, 15–17]. The constants of the ADP association with Ca^{2+} ions exceed the corresponding values for the bonds with Na^+ ions by almost two orders of magnitude. (For the equilibrium constants of the reactions M + $ADP^{3-} \leftrightarrow MADP^{(3-n)-}$, where M is a metal ion and n is its valence, the values of log$K$ are 3.08 and 1.12, respectively [20].) However, the results obtained for the photosystems in this work flatly contradicted the assumption of a possible increase in the yield of H_2O_2.

In all of the analyzed cases, adding $CaCl_2$ to AX + NaCl solutions leads to a considerable drop in the yield of H_2O_2 (Table 1, Fig. 3). There is no correlation between the amount of the produced hydrogen peroxide and any of the components of the recorded EPR spectra. However, there does seem to be a correlation between the total Int of the EPR signals and the yield of H_2O_2 (Fig. 3). In solutions of Ado + NaCl, the yield of H_2O_2 in both the presence and the absence of $CaCl_2$ falls greatly upon an increase in the Int of the EPR signals. This in turn is due to an increase in the salt content (Table 1, Fig. 3). At the same content of AX, NaCl, and the $CaCl_2$ additive, the drop in the yield of H_2O_2 in the presence of $CaCl_2$ is 1.6–3.3 times smaller in the Ado solutions than in the ADP solutions. The yield of H_2O_2 in Ado solutions containing Ca^{2+} exceeds the yield of H_2O_2 in similar ADP solutions by

a factor of 1.5–7.5, depending on the content of salts in the solutions: 0.1 M NaCl, 0.01 M $CaCl_2$ and 1×10^{-3} M NaCl, 2×10^{-4} M $CaCl_2$, respectively.

The drop in the formation of H_2O_2 in the AX solutions containing $CaCl_2$ could obviously be due to the particular nature of the bonding between Ca^{2+} ions and Ado. In addition to the phosphate groups of nucleotides, which are the main centers for bonding metal cations [21], the hydroxyl groups of ribose and endocyclic nitrogen atoms N7, N1, and N3 of the base are also possible centers of their bonding (according to crystallographic data) [21]. It is assumed that the donor nitrogen atoms of the base and hydroxyl groups of ribose play no notable role (according to NMR) in bonding nucleotides with Mg^{2+} ions, the properties of which are similar to those of Ca^{2+} ions [22]. Nevertheless, it has been shown by means of $^1H-^{15}N$ HMBC that N1 atoms of the adenine fragment of ATP interact with Mg^{2+} ions in the pH range of ~2.5–5.0 [23]. ^{31}P NMR shows that phosphate groups also bond Mg^{2+}. Diffusion measurements of ^1H indicate that only one ligand and one Mg^{2+} ion participate in ATP-Mg complexes. Alkalizing the solution to pH ~ 7 reduces (but does not completely eliminate) the ^{15}N chemical shift observed in the presence of Mg^{2+}. This indicates the participation of N1 atoms in the interaction with metal ions. It should be noted that these experiments were performed at very high concentrations of ATP (0.2 M) where the concentration of ATP associates was high. (With no Mg^{2+}, it is more than 6×10^{-2} M when $K_{sa2} = 1.3$ M^{-1} [11] is used in calculations, and ~0.2 M when using $K_{sa2} = 8000$ M^{-1} and $K_{saN} = 50$ M^{-1} in [9].) However, we believe that when a change in the ^{15}N chemical shift is induced by the self-association of the nucleotide, the changes cannot be selective for the N1 atom. Complexes of nucleotides with metals are thought to be outer-sphere complexes in which the bonds between metal ions and the nitrogen of heterocycles are formed through molecules of H_2O [24].

Analysis of the EPR spectra reveals no systematic change in the Int of the signals, or in the relative content of their components when $CaCl_2$ is added to the irradiated solutions before they are frozen (Table 1). In the presence of $CaCl_2$, however, there is always a drop in the total relative content of the $HO_2^{\bullet}$ and $AOH^{\bullet}$ radicals. (With the pairwise summation of the relative content of other different components of the S signals, no unidirectional change is observed when $CaCl_2$ is added to the solutions).

The possibility of hydroxide ions being near photoinduced reaction centers is important for the formation of $HO_2^{\bullet}$ and $AOH^{\bullet}$ radicals [1, 2]. At a relatively high content of AX (1×10^{-3} M), interaction between electron-deficient centers and the OH^- that accumulates on a sample's surface is possible, due to the opacity of the samples [25]. However, a fivefold reduction in [AX] visibly leads to greater transparency of the samples, which probably means the impact of this factor becomes smaller. On the other hand, it was proposed in [2–4] that the formation of hydroxide ions in the weakly acidic pH range of 4–6.5 is possible with the protonation of photoinduced triplet states of AX by H_2O molecules, since the pK_a values for purines in the ground state are lower than those for purines in the triplet state [26, 27]. Unfortunately, since we do not know the data on the changes in the characteristics of the photoexcited triplet states of AX complexes with divalent metals, we cannot draw conclusions on the possibility of this path of the formation of hydroxide ions in ADP complexes with Ca^{2+}.

The conformational changes that affect the glycosidic bonds of ATP molecules in the presence of Mg^{2+} are shown in [28]. In principle, such changes in the conformation of the investigated AX in the presence of Ca^{2+} ions could considerably affect the structure of the frozen aggregates. The ionic radius of Ca^{2+} greatly exceeding that of Mg^{2+} is also likely to be a significant factor in this effect.

In [1, 2], it was suggested that the unique ability of AX to photoproduce H_2O_2 could play an important role in the processes of evolutionary biochemistry. The data on the inhibition of the H_2O_2 photoproduction by Ca^{2+} ions generally do not contradict the suggested role of AX, since the $[Ca^{2+}]/[Na^+]$ ratio of 0.1–0.2 used in this work is much higher that the $[Ca^{2+}]/[Na^+]$ ratio in seawater: ~0.02 [29].

ACKNOWLEDGMENTS

The authors thank E.N. Degtyarev for his great help in this work.

REFERENCES

1. T. A. Lozinova, A. V. Lobanov, and A. V. Lander, Russ. J. Phys. Chem. A **89**, 1492 (2015).
2. T. A. Lozinova, A. V. Lobanov, and A. V. Lander, Russ. J. Phys. Chem. A **90**, 2297 (2016).
3. T. A. Lozinova and A. V. Lander, Biophysics **58**, 341 (2013).
4. T. A. Lozinova and A. V. Lander, Russ. J. Phys. Chem. A **88**, 163 (2014).
5. K. Kobayashi, J. Phys. Chem. B **114**, 5600 (2010).
6. A. V. Lobanov, N. A. Rubtsova, Yu. A. Vedeneeva, and G. G. Komissarov, Dokl. Chem. **421**, 190 (2008).
7. L. Soccorsi and M. Cignitti, Bioelectrochem. Bioenerg. **9**, 219 (1982).
8. J. Morcillo, E. Gallego, and F. Peral, J. Mol. Struct. **157**, 353 (1987).
9. F. Peral and E. Gallego, Biophys. Chem. **85**, 79 (2000).
10. D. A. Beshnova, A. O. Lantushenko, D. B. Davies, and M. P. Evstigneev, J. Chem. Phys. **130**, 165105 (2009).
11. K. H. Scheller, F. Hofstetter, P. R. Mitchell, et al., J. Am. Chem. Soc. **103**, 247 (1981).

12. K. H. Scheller and H. Sigel, J. Am. Chem. Soc. **105**, 5891 (1983).
13. R. Tribolet and H. Sigel, Eur. J. Biochem. **170**, 617 (1988).
14. K. E. van Holde and G. P. Rossetti, Biochemistry **6**, 2189 (1967).
15. R. B. Martin, Chem. Rev. **96**, 3043 (1996).
16. H. Sigel, R. Tribolet, R. Malini-Balakrishnan, and R. B. Martin, Inorg. Chem. **26**, 2149 (1987).
17. B. I. Sukhorukov, I. Ya. Gukovsky, A. I. Petrov, et al., Int. J. Quantum Chem. **17**, 339 (1980).
18. V. Kleinwächter, Collect. Czech. Chem. Commun. **371**, 1622 (1972).
19. *Physico-Chemical Properties of Nucleic Acids,* Ed. by J. Duchesne (Academic, London, 1973), p. 119.
20. R. M. Smith, A. E. Martell, and Y. Chen, Pure Appl. Chem. **63**, 1015 (1991).
21. W. Saenger, *Principles of Nucleic Acid Structure* (Springer, New York, 1987).
22. Z. Szabó, Coord. Chem. Rev. **252**, 2362 (2008).
23. L. Jiang and X.-A. Mao, Spectrochim. Acta A **57**, 1711 (2001).
24. E. M. Bianchi, S. A. A. Sajadi, and H. Sigel, Chem. Eur. J. **9**, 881 (2003).
25. S.-C. Park, E.-S. Moon, and H. Kang, Phys. Chem. Chem. Phys. **12**, 12000 (2010).
26. J. J. Aaron and J. D. Winefordner, Photochem. Photobiol. **18**, 97 (1973).
27. J. W. Longworth, R. O. Rahn, and R. G. Shulman, J. Chem. Phys. **45**, 2930 (1966).
28. L. Jiang and X.-A. Mao, Polyhedron. **21**, 435 (2002).
29. H. Trinks, W. Schroder, and C. K. Biebricher, Origins Life Evol. Biosphere **35**, 429 (2005).

Translated by Yu. Modestova